

A Numerical Simulation Model of Land and Sea Breezes on the Sirte Gulf, Libya

نموذج تحليل عددي لمحاكاة ظاهرة نسيم البر والبحر في خليج سرت، ليبيا

عبد الحليم علي المحي

Dr. Abdul-Haleem A. Al-Muhyi

Meteorology Department, Collage of Science, Alfateh-University, P.O Box 13486, Tripoli, Libya, e-mail:th67abdul@yahoo.com

جامعة الفاتح، كلية العلوم، قسم الأرصاد الجوية

Abstract: A numerical model is developed in order to simulate land and sea breeze phenomenon in the Gulf of Sirte, which is located on the Libyan coastline. A Mixed-Layer Model is used to simulate land and sea breezes and their effect on the coastal strip. The model consists of three layers: the surface layer, the mixed layer and the stable layer. The primitive equations are averaged in the mixed layer to yield prediction equations for the horizontal components of the wind, two components of the horizontal pressure gradient, potential temperature of the mixed layer, the height of the base of the overlying stable layer and the surface temperature. The results show that the model is successful in simulating land and sea breezes and making clear the difference between the influence of onshore and offshore winds on the coastal strip.

Keywords: Sirte Gulf, Libya, Land and Sea breezes, Numerical model, Mixed Layer Models, Simulate

المستخلص: يهتم البحث بتطوير نموذج عددي يماثل ظاهرة نسيم البر والبحر، خلال فصل الصيف والشتاء في خليج سرت، على الساحل الجنوبي للبحر المتوسط في ليبيا، وذلك باستخدام (نموذج طبقة الخلط) والذي يتكون من ثلاثة طبقات هي، السطحية، الخلط، والطبقة المستقرة. أستخدمت معادلات أولوية في طبقة الخلط. ومنها تم الحصول على معادلات التنبؤ بالمركبات الأفقية للرياح على طول المحور (X) والمحور (Y) إضافة إلى معادلات التنبؤ بمركبات إنحدار الضغط الأفقي باتجاه المحور (X) والمحور (Y) كما أمكن التنبؤ بدرجة الحرارة الجهدية لطبقتي الخلط، وإرتفاع قاعدة الطبقة المستقرة، فضلاً عن التنبؤ بدرجة حرارة سطح الأرض. وعليه برهنت النتائج مدى التماثل لنسيمي البر والبحر، وإمكانية التعرف على صفات، وتأثير الرياح التي تهب ومن وإلى البحر.

كلمات مدخلة: خليج سرت، ليبيا، نسيم بر وبحر، قياس تماثل، نموذج طبقة الخلط.

Introduction

The location of Libya on the Southern coast of the Mediterranean Sea, with a coastline extending about 1850 kilometers (1131 miles), has had a great effect upon the ethnography (Salem Ali,1967) as most of the Libyan people live on the coastal strip and their activities related to agriculture, fishing and other things concentrate in the area of coastal strip. The coast is under the effect of land and sea breezes which taken together constitute a diurnal analog of monsoon circulation. They occur due to thermal contrast between land and sea surface water of the Mediterranean Sea. Although the sea breeze is a relatively common phenomenon and has an analogous mechanism throughout space, it has

different effects and characteristics from place to place, coinciding with geographic location (water body and land whether desert or covered by vegetation) Thus, studying land and sea breeze phenomenon is regarded as very important given for the location of Libya. In this paper we will study sea and land breezes by using a numerical simulation model. We apply this model on the coastal strip of the Sirte Gulf as a sample of the Libyan coast.

The Sirte Gulf (Fig.1) itself exhibits a very large, concave appearance within the Libyan coast. It extends from latitude 32°:55' N, on the Northern edge of Libya, to latitude 30°:15' N. on the Southern edge of the Gulf. It has a length of about 270 kilometers (167.4 miles) from East to West, (long. 15°:10' to 20°:5' East) and a width of,

approximately, 165 kilometers (103 miles) from North to South, including a coastline approaching 700 kilometers (434 miles) long. (Salem,1967).

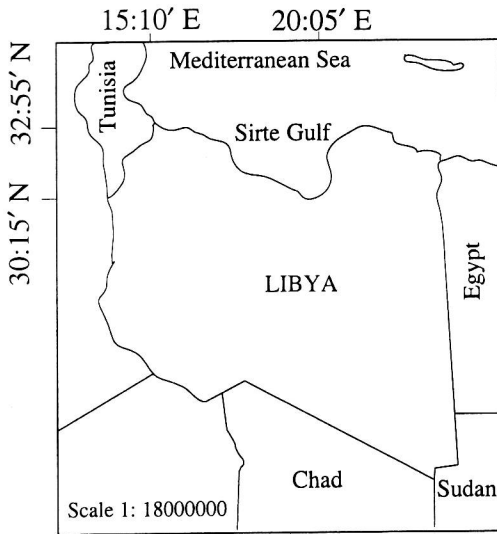


Fig. (1) Libya map (Libyan School Atlas)

Materials and Methods

● Model Description

In this study a mixed layer model has been used which is based on the mixed layer concept described by (Lavoie 1972). This model is based on a well mixed layer atmosphere which is present

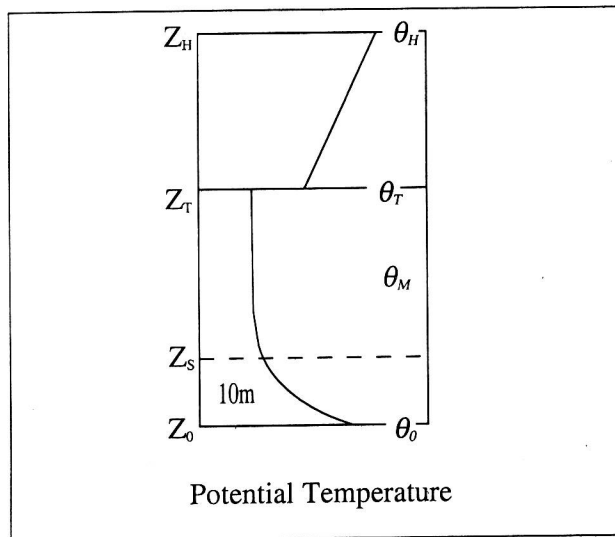


Fig. (2) Thermal structure assumed in the model

in the lower (1-2 km) of the troposphere. The model atmosphere consists of three layers defined by their distinctive lapse rates of potential temperature as shown in Fig.(2).

The lower most layer is the surface layer, which is parameterized with a fixed depth of 10m and contains most of the wind shear. (Z_0) is the height of the ground surface. The middle layer starts from the top of the surface layer (Z_s) to the bottom of the

stable layer (Z_T). This layer is well mixed so the temperature and the horizontal wind are approximately constant in height. The uppermost layer is approximated as a deep stratum layer of constant stable lapse rate (Lavoie 1972). (Z_H) is the level where the mesoscale perturbation in potential temperature produced by surface heating or topography is assumed to vanish, (Keyser and Anthes,1977).

● Model Equations

A set of predictive equations are used to predict seven dependent variables: two horizontal components of wind vector along (x, y) axes, two components of horizontal pressure gradient along (x, y) axes, the potential temperature of the mixed layer, the height representing the top of the mixed layer, and surface temperature (using the force restore method, (Deardorff 1978).

These variables are: (u) is the zonal wind, (v) is the meridional wind, (Z_T) is the height of the mixed layer, (θ_M) is the potential temperature of the mixed layer, (p_x) is the horizontal pressure gradient along the (x) axis, (p_y) is the horizontal pressure gradient along the (y) axis and (θ_0) is the surface temperature.

The predictive equations for the horizontal wind are the momentum equations for (x) and (y) as follows:

$$\left[\frac{\partial u}{\partial t} = -u \frac{\partial u}{\partial x} - v \frac{\partial u}{\partial y} + f v - \alpha \frac{\partial p}{\partial x} - \frac{C_D |W| u}{(Z_T - Z_s)} + K_x \frac{\partial^2 u}{\partial x^2} + K_y \frac{\partial^2 u}{\partial y^2} \right] \quad (1)$$

$$\left[\frac{\partial v}{\partial t} = -u \frac{\partial v}{\partial x} - v \frac{\partial v}{\partial y} - f u - \alpha \frac{\partial p}{\partial y} - \frac{C_D |W| v}{(Z_T - Z_s)} + K_x \frac{\partial^2 v}{\partial x^2} + K_y \frac{\partial^2 v}{\partial y^2} \right] \quad (2)$$

For both equations, the first two terms, on the right hand side are, the horizontal advection terms along (x) and (y) respectively, the third term is, the Coriolis force, the fourth term is the pressure gradient force, the fifth term is the frictional term where (C_D) is the drag coefficient. (Lous *et al.* 1981) suggested to computed:

$$\left[C_D = C_N \left[1 + 10R_i / (1 + 5R_i)^{1/2} \right] \quad , R_i > 0 \right. \\ \left. C_D = C_N = \left[k / \ln(Z_s/Z_0) \right]^2 \quad , R_i \leq 0 \right]$$

$$\text{where: } R_i = Z_s(\epsilon) \theta_m / [T_0 / |W|]^2$$

and (R_i) Richardson number:

$$\text{Where } |W|^2 = u^2 + v^2$$

- (u, v) = the horizontal components of the wind along (x) and (y), respectively.
- (k) = von Karman constant (0.4).
- (Z₀) = roughness length (0.001) for desert (Stull, 1988).

(Charnock, (1955), suggests that (Z₀) varies with the turbulent stress over water and so we set

$$(Z_0) = 10^{-4} |W|^2 / g$$

(W) the absolute value of horizontal wind.

The sixth and seventh terms are, horizontal mixing terms where (K_x) and (K_y) represent the horizontal diffusion coefficients for both components.

The pressure gradient force adopted in this study is that formulated by (Keyser and Anthes, 1977) as follows:

$$\begin{aligned} -\alpha \frac{\partial p_x}{\partial x} &= f_v g + \frac{g(z_H - z_T)}{2\theta_M} \left[\frac{\partial \theta_H}{\partial x} + \frac{\partial \theta_T}{\partial x} - \gamma_s \frac{\partial z_T}{\partial x} \right] - g \left[\frac{\theta_T - \theta_M}{\theta_T} \right] \left[\frac{\partial z_T}{\partial x} \right] + \left[\frac{g(z_T - z_s)}{2\theta_M} \right] \left[\frac{\partial \theta_M}{\partial x} \right] \\ -\alpha \frac{\partial p_y}{\partial y} &= -f_u g + \frac{g(z_H - z_T)}{2\theta_M} \left[\frac{\partial \theta_H}{\partial y} + \frac{\partial \theta_T}{\partial y} - \gamma_s \frac{\partial z_T}{\partial y} \right] - g \left[\frac{\theta_T - \theta_M}{\theta_T} \right] \left[\frac{\partial z_T}{\partial y} \right] + \left[\frac{g(z_T - z_s)}{2\theta_M} \right] \left[\frac{\partial \theta_M}{\partial y} \right] \end{aligned} \quad (3)$$

where (u_g) and (v_g) are the geostrophic wind components prescribed at the upper limit (Z_H) of the model. At the top of the mixed layer, the vertical

$$\left[w_T = -\frac{\partial u}{\partial x} (z_T - z_s) - \frac{\partial v}{\partial y} (z_T - z_s) + w_s \right] \quad (5)$$

velocity can be expressed as:

$$\left[w_s = u \frac{\partial z_s}{\partial x} + v \frac{\partial z_s}{\partial y} \right] \quad (6)$$

where (w_s) is the vertical velocity at the surface.

$$\left[\frac{\partial z_T}{\partial t} = -u \frac{\partial z_T}{\partial x} - v \frac{\partial z_T}{\partial y} + w_T + \left[\frac{1}{\gamma_s} \left(\frac{\partial \theta}{\partial t} \right) \right] \right], \theta_M \geq \theta_T \quad (7)$$

The prognostic equation for the height of the top of the mixed layer (Z_T) is:

The first two terms on the right hand side are, the horizontal advection terms, and the third term is, the vertical velocity of the top of the mixed layer. The last term is, a provision for an increase in the value of (Z_T), and the brace is used to emphasize that the term is to be included only when (θ_M ≥ θ_T).

The prognostic equation for the potential temperature at the mixed layer is written as:

$$\left[\frac{\partial \theta_M}{\partial t} = -u \frac{\partial \theta_M}{\partial x} - v \frac{\partial \theta_M}{\partial y} + \frac{C_{DT} |W|}{Z_T - Z_s} (\theta_s - \theta_M) + \frac{\partial}{\partial x} \left[K_x \frac{\partial \theta_M}{\partial x} \right] + \frac{\partial}{\partial y} \left[K_y \frac{\partial \theta_M}{\partial y} \right] \right] \quad (8)$$

The first two terms on the right hand side are, the horizontal advection terms. The third term represents, the effect of the flux of heat from the

surface to the atmosphere, or vice versa where (C_{DT}) is the drag coefficient for the surface heat flux which is computed by (Lous *et al.* 1981):

$$\left[C_{DT} = C_N / \left[1 + 15 R_i (1 + 5 R_i) \right]^{1/2} \right], R_i > 0$$

$$\left[C_{DT} = C_N \left[1 - 15 R_i / \left[1 + 75 C_N (-R_i Z_s / Z_0) \right]^{1/2} \right] \right], R_i \leq 0$$

(θ₀) is the potential temperature at the surface. The fourth and fifth terms are, horizontal mixing terms. Computing and predicting the land surface temperature is based on the force restore method (Deardorff, 1978). The equation for the force restore method is:

$$\left[\frac{\partial T_0}{\partial t} = -2 \Pi^{1/2} H_A / (\rho_s C_s d) - 2 \Pi (T_s - T_g) / \tau \right] \quad (9)$$

where (ρ_s) is the soil density, (C_s) is the specific heat of the soil, (T_g) is the constant temperature at the bottom (10 cm), (π) is the diurnal period, (d) is the depth of the soil slab and (H_A) is the net flux of heat. The sea surface temperature is assumed to be constant during the day.

These predictive equations represent the simple Mixed Layer Model of (Lavoie, 1972). In (Al-Muhyi, 1998), the application of this model gave unrealistic results in simulating local wind. He found that during night time, strong local wind still prevails and wind speed reduces very slowly, and this is inconsistent with the cycle of local wind. It is well known that the land cools at night and eradicates the pressure gradient, so the local wind weakens and wind speed gradually reduces after mid-night, and the wind becomes calm or near calm. For this reason and for the model to become realistic, he extended the model to include a model assumption term so that equations (1) and (2), the momentum equations to predict horizontal wind components (u) and (v) along (x) and (y) axes are now written as:

$$\left[\frac{\partial u}{\partial t} = -u \frac{\partial u}{\partial x} - v \frac{\partial u}{\partial y} + f_v - \alpha \frac{\partial p}{\partial x} - \frac{C_D |W| u}{(Z_T - Z_s)} + \frac{2 C_D |W|}{Z_T - Z_s} (u_g - u) + K_x \frac{\partial^2 u}{\partial x^2} + K_y \frac{\partial^2 u}{\partial y^2} \right] \quad (10)$$

$$\left[\frac{\partial v}{\partial t} = -u \frac{\partial v}{\partial x} - v \frac{\partial v}{\partial y} - f_u - \alpha \frac{\partial p}{\partial y} - \frac{C_D |W| v}{(Z_T - Z_s)} + \frac{2 C_D |W|}{Z_T - Z_s} (v_g - v) + K_x \frac{\partial^2 v}{\partial x^2} + K_y \frac{\partial^2 v}{\partial y^2} \right] \quad (11)$$

● The finite difference formulation of the model

A rectangular integration domain is used in this model. The grid network consists of (38) points along the (x) axis and (42) points along the (y)

axis. The grid spacing is (15km) for both (x) and (y), making it a horizontal square grid system.

All predicted variables as

- * Horizontal wind velocity (u,v) along (x,y) axis
- * Mixed layer potential temperature (θ_m)
- * Depth of mixed layer (θ_T)
- * The surface temperature (θ_o)

are determined at each grid point. The vertical velocity (w) and the atmospheric pressure (p), are also determined at each grid point. The space derivatives in the advection terms are calculated using the upstream difference analogue. For other space derivatives, the centered method of finite differencing scheme is used.

● Application of the model

The model is numerically integrated to study the diurnal variation of sea breezes on Sirte Gulf. We applied the model twice, to simulate sea and land breezes during the Summer and Winter Seasons.

It is worth mentioning that we selected for the Summer season the month of August, since it is the hottest month in the region of Sirte Gulf. During this month, the temperature contrast between land and water is maximum, and strong sea breezes typically develops. For the Winter season we selected the month of January, which is the coldest month.

● Simulations of land and sea breeze

In these simulations, the physical characteristics of land and sea breezes are investigated. The constant parameters used in this model for all integrations are presented in (table 1).

Table (1) The constant parameters used in the numerical model

$F = 7.9431 \times 10^{-5} \text{ s}^{-1}$	Coriolis parameter at 33°N
$g = 9.8 \text{ m/s}^2$	Acceleration due to gravity
$\rho = .0012 \text{ g/cm}^3$	Air density
$Z_0 = 0.001 \text{ m}$	Roughness length for desert
$\gamma_d = 0.00975 \text{ }^\circ\text{K/m}$	Adiabatic lapse rate
$\gamma_s = 0.0075 \text{ }^\circ\text{K/m}$	Assumed lapse rate at the stable layer
$k = 0.4$	Van Karman constant
$\rho_s = 2.65 \text{ g/cm}^3$	The soil density
$C_s = .24 \text{ J/g }^\circ\text{K}$	The specific heat of the soil
$\pi = 1440 \text{ min}$	The durnal period
$d = 10 \text{ cm}$	The depth of the soil slab.
$\Delta x = 15000 \text{ m}$	Grid distance along x axis
$\Delta y = 15000 \text{ m}$	Grid distance along y axis
$\Delta t = 360 \text{ sec}$	Time step increment

Series of experiments has been done to simulate land and sea breezes, as accurately as possible, with observational data (Table 2). To accomplish this purpose, several integrations of the model have been done using different variables, which are similar to the observational data, except the surface temperature for land and water where real data were used. The observational data were taken from the station of Misurata City, located on 32°, 19' Lat. N. and 15°, 03' Long.E.

Table (2) Observational data which represent monthly mean wind speed and direction taken from station of Misurata.

	Time GMT	300	600	900	1200	1500	1800	2100	2400
	Time LOC	500	800	1100	1400	1700	2000	2300	200
August	Wind speed (knot)	4.7	4.2	5.3	7.3	10.3	12	10.2	7.6
	wind direction	349	351	310	333	355	1	6	3
January	Wind speed (knot)	6.8	7.1	7.8	8.5	9.1	6.8	7.9	7.3
	wind direction	243	256	239	252	299	305	286	260

Results of Simulation

The model has been applied to simulate land and sea breezes on the Sirte Gulf. The model is integrated for 24 hours of real time for each season. The initial time corresponds to (06:00 am) local time. We assume that the atmosphere of the domain is calm (prevailing wind is zero). The results gotten from the model are presented in the form of computer plots, (44) figures, showing the resulting one hour interval integrations. These figures show the initial evolution, and subsequent development of land and sea breezes, in response to differential heating of the earth's surface. We have selected only (18) figures in this paper for two seasons. Following the series of these figures, we can see the course of land and sea breeze development.

(I) During Summer Season

In the summer season, the first (4 hours), a sea breeze has not yet started to blow, because the temperature contrast between land and water is still not adequate for the thermal wind to develop. At time (11:00 am) the onshore wind starts to blow with primary maximum speed of (4 knots) as show in Fig (3).

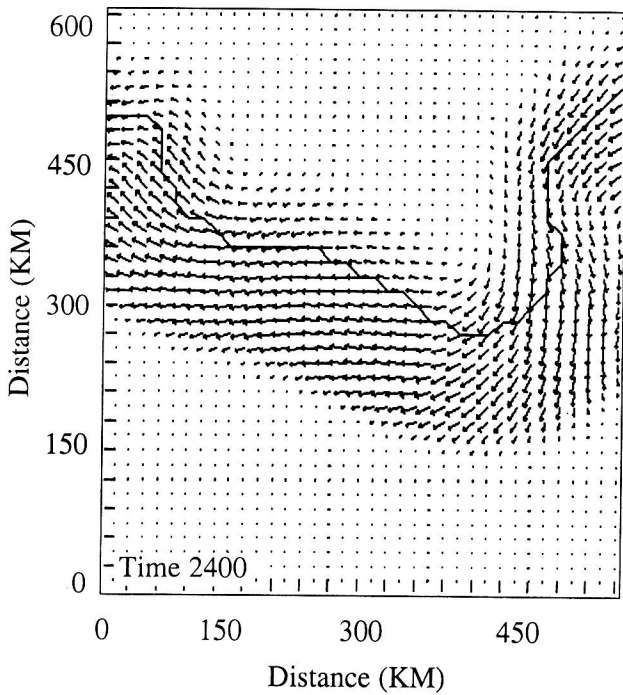


Fig. (3) Maximum wind speed (4 knots).

At time (13:00) or (1:00 pm), the sea breezes increase to a maximum speed (6.8 knots), and spreads inland, at a right angle, to the coastlines. In this figure, we can note that, the geometry of the coastlines has a major effect on the distribution of the sea breeze.

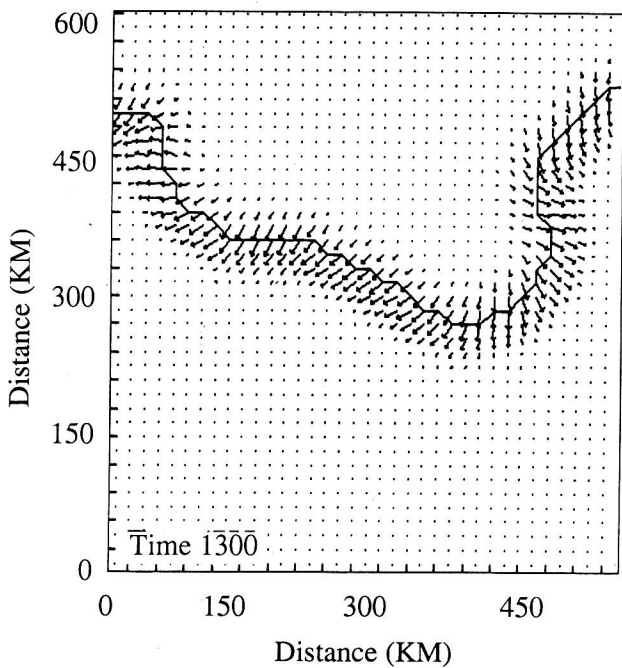


Fig. (4) Maximum wind speed 6.8 knots

When the coasts are straight, a uniform sea breeze spreads inland, and when the coasts are not straight, the sea breeze is not uniform. Looking at Figures (5 and 6), which represent time (15:00 and 17:00) or (3:00 and 5:00 pm), we see that the sea

breeze has penetrated inland much farther, and the wind is now blowing over the sea near the coastlines.

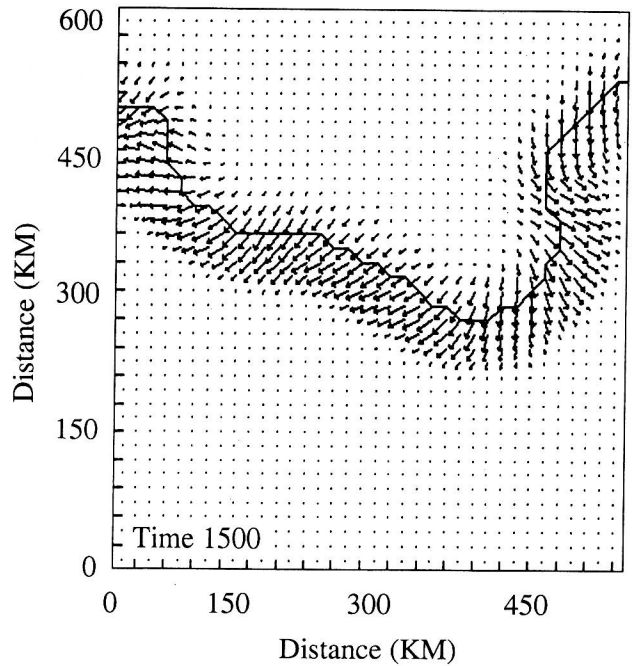
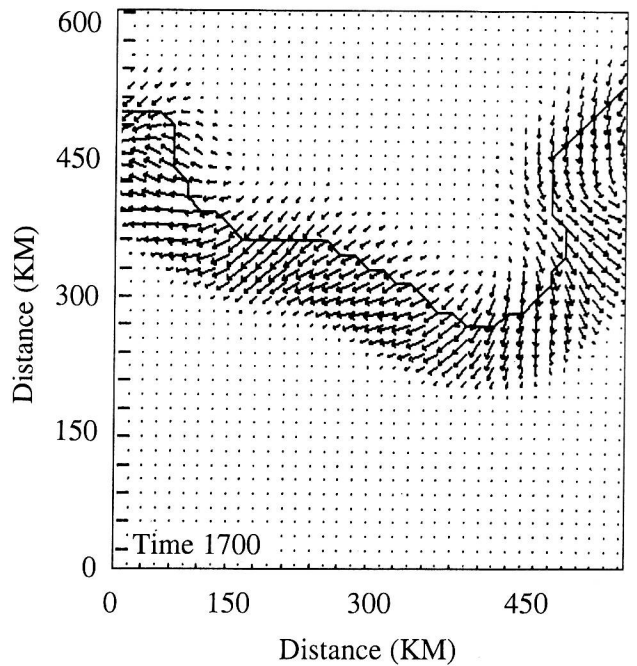


Fig. (5) Maximum wind speed (9 knots).



(6) Maximum wind speed (9.8 knots).

Subsequent figures show that the sea breeze increases gradually to reach its maximum value at about (19:00 or 7:00 pm), three hours after the time at which the temperature difference between land and water reaches the maximum at about (16:00 or 4:00 pm).

This is consistent with the finding of (Haurwitz Simpson, 1994).

Fig. (8,9,10) show that, at nighttime, the onshore breeze still prevails, but of reduced intensity.

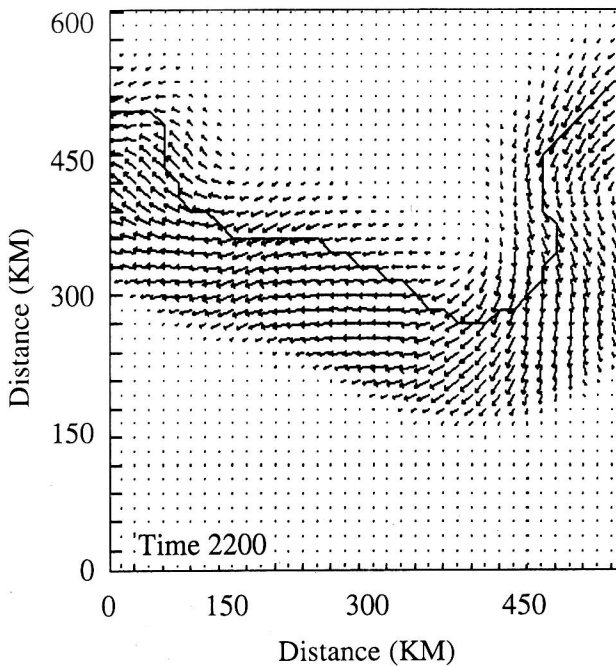


Fig. (8) Maximum wind speed (6.4 knots).

Its speed gradually decreases, and it penetrates inland for a distance of about (100 km) at time (24:00 to 02:00 am or 12:00 to 02:00am) as shown in (Fig.9).

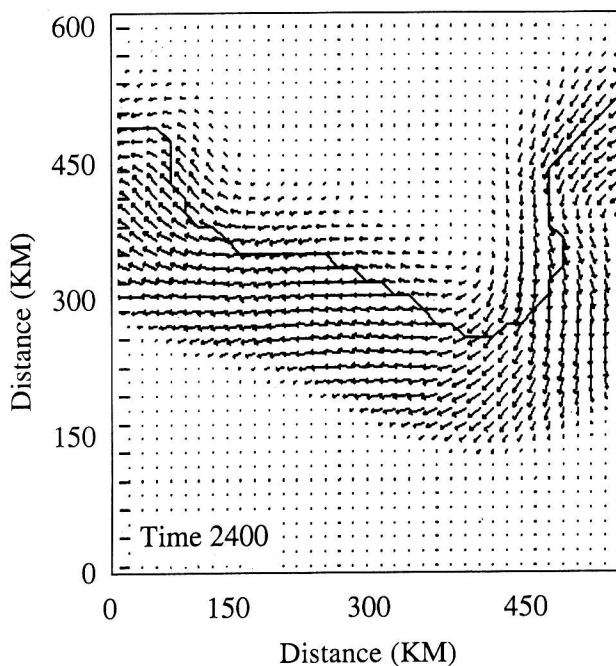


Fig. (9) Maximum wind speed (4.5 knots).

By midnight, land air starts to cool to eradicate the sea breeze pressure difference, and the air over coastlines is consequently about calm Fig.(10).

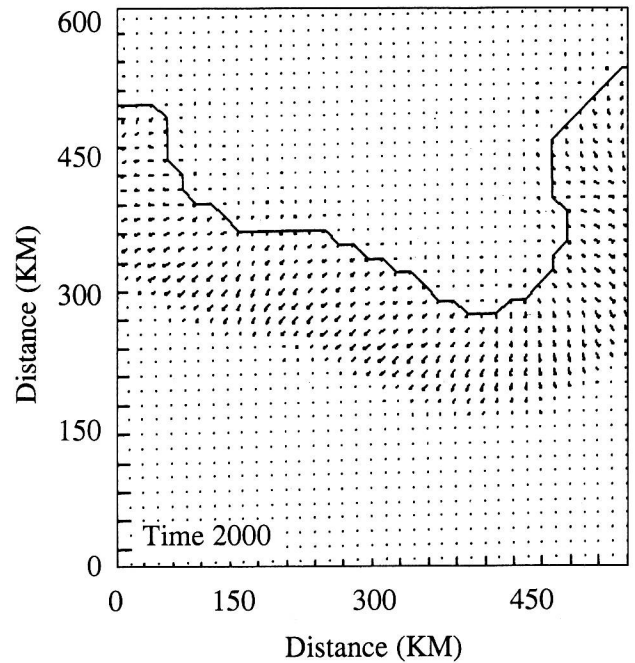


Fig. (10) Maximum wind speed (3 knots).

After (03:00 am), the wind over coastlines dies down, while it still prevails away from coastlines until the early hours of the next day. We also noted that the direction of the sea breeze does not remain constant in the course of the day. It gradually veers in a clockwise direction, until by late evening, it is blowing nearly parallel to the coastlines.

One of the important results we can note is that, there is no land breeze blow during the Summer season. This is because the diurnal temperature of the earth's surface is higher, or approximately, equal to water temperature, and therefore, this leads to pressure on the water being higher, or approximately, equal to that on the land.

(II) During Winter season.

In the Winter season, we can see in the first hour of the model, there is no wind blowing, but at time (07:00 am) in the morning, the offshore wind starts to blow and gradually increases its speed with time (See Fig.11).

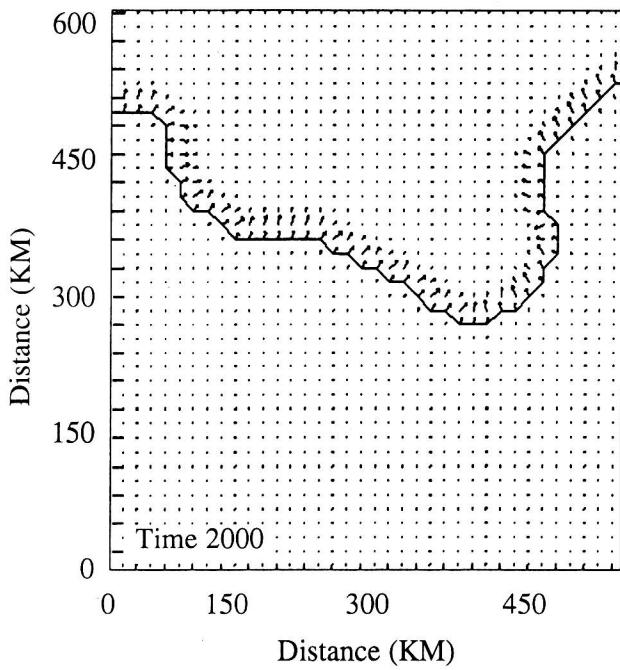


Fig. (11) Maximum wind speed (3.3 knots).

In Fig.(12) we see a maximum wind speed of (5.3 knots), which spreads on water, instead of inland in Summer season, as mentioned before, at a right angle to coastlines.

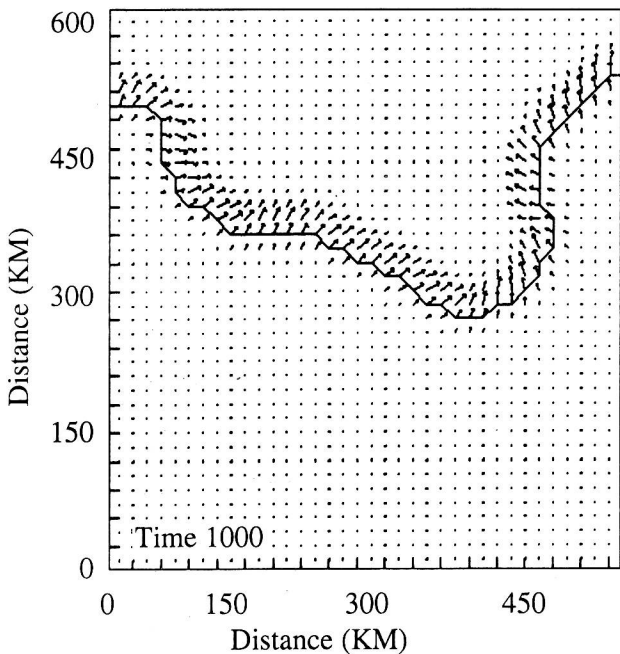


Fig. (12) Maximum wind speed (5.3 knots).

The geometry of the coastlines has a major effect on the distribution of land breeze. When the coasts are straight, a uniform land breeze spreads on water, and when coasts are not straight, the land breeze is not uniform. We can see in (Fig.13) a maximum wind speed of (7.3 knots), and slightly changes its direction to the left, and penetrates on water farther to reach about (70km).

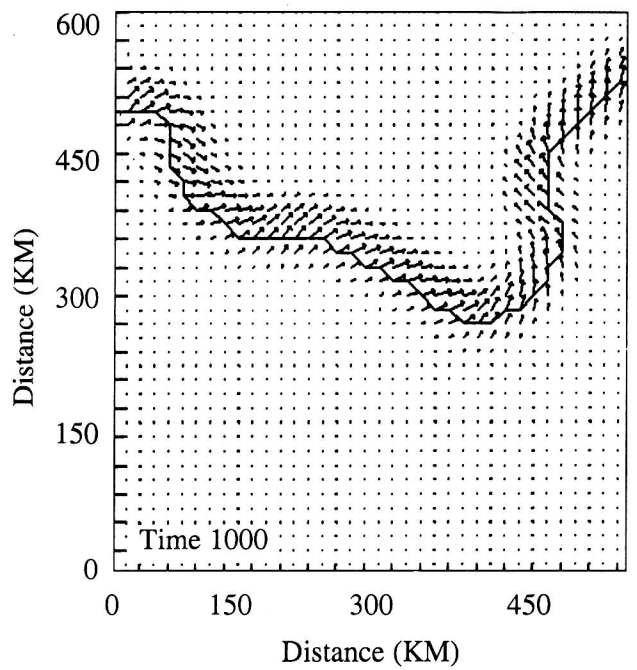


Fig. (13) Maximum wind speed (7.3 knots).

In Figure (14) we note a maximum speed of (8.2) knots. The direction now is, approximately, parallel to the coastlines, and the wind is blowing over the land near the coastlines.

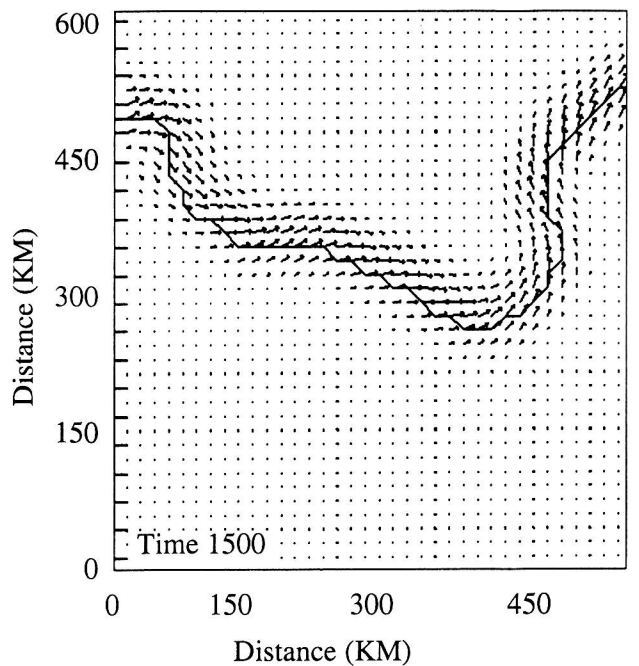


Fig. (14) Maximum wind speed (8.2 knots).

In Fig. (15), we note that, the wind speed is reduced to (7.2 knots), and at some points of the coastlines, it is still parallel, whereas in other points, it becomes onshore. In subsequent figures, onshore wind is more pronounced with more reduced intensity.

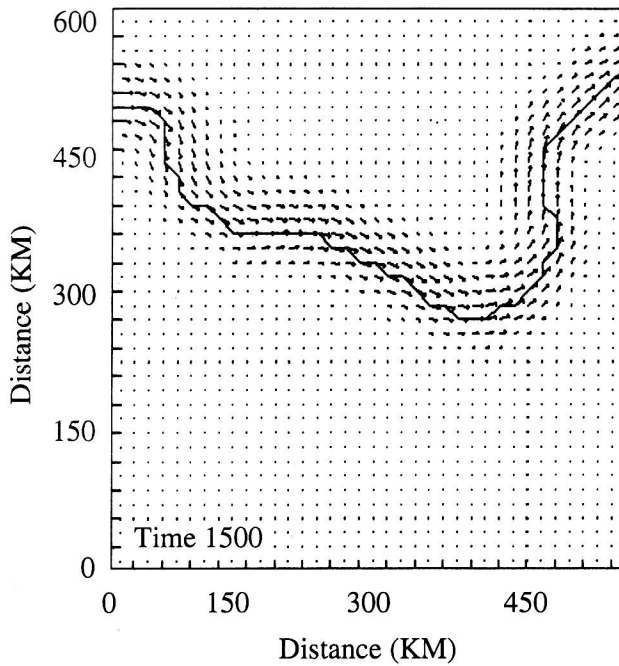


Fig. (15) Maximum wind speed (7.2 knots).

At time (21:00 or 9:00 pm), (Fig. 16), the wind becomes completely onshore with a maximum wind speed of (6 knots).

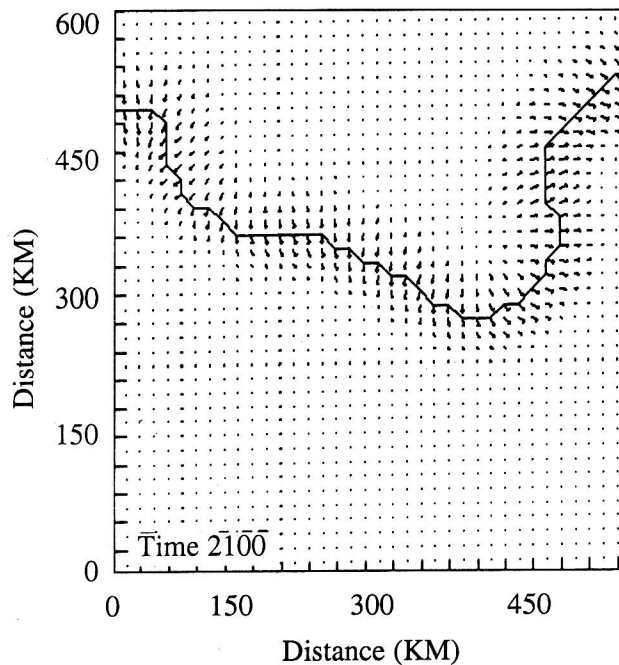


Fig. (16) Maximum wind speed (6 knots).

The deflection in the wind direction, from offshore during daytime, to onshore at nighttime, is due to the increase in the earth's surface temperature during daytime, which exceeds water temperature from time (14:00 to 20:00 or 2:00 pm to 8:00 pm), and this in turn changes the pressure gradient to become from water to land. In Fig. (17) and (18), we

can see the wind withdraw its force, and gradually begin to die away.

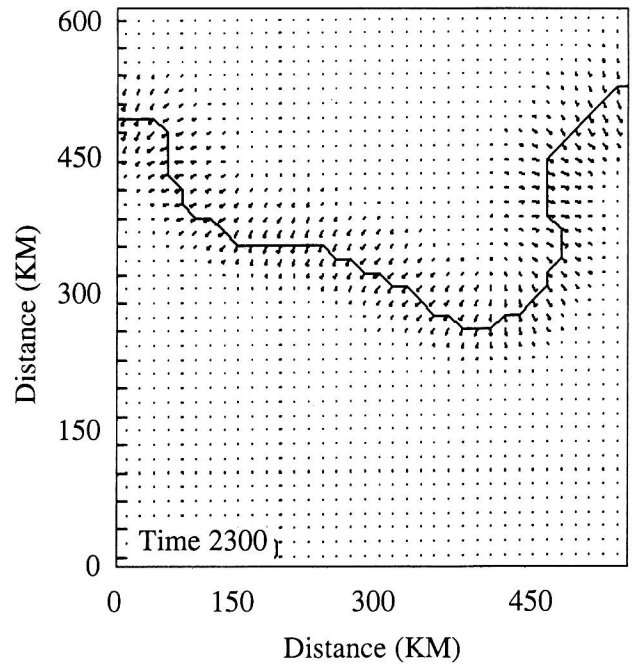


Fig. (17) Maximum wind speed (3.6 knots).

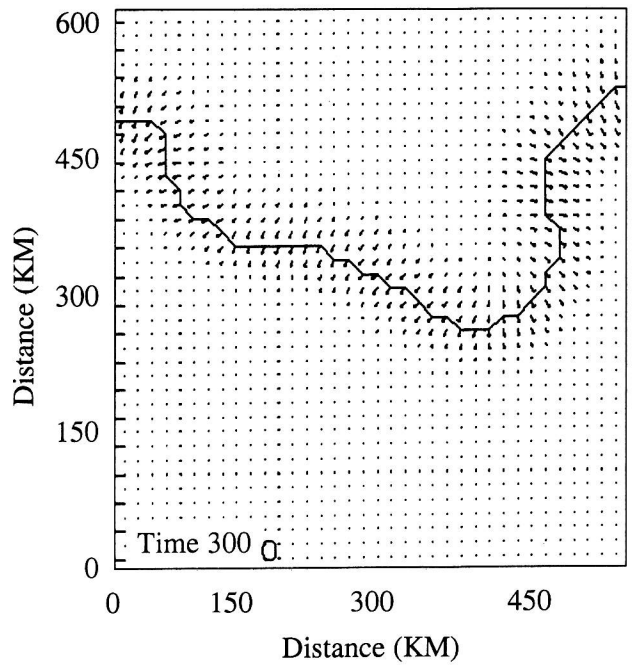


Fig. (18) Maximum wind speed (2.8 knots).

We note that, during this season (Winter), in the course of day, land and sea breezes are blowing while in Summer season, land breeze is seldom blowing.

Conclusions and Results

A mesoscale model, represents the atmosphere by three layers has been developed. The lower most layer in contact with the ground, is the surface layer, the middle layer, is a mixed layer, which is homogeneous in its vertical distribution of potential temperature. This layer is delineated at its upper boundary by a stable layer.

The model was integrated several times, until it simulates sea and land breezes consistent with observational data, during the Summer and the Winter seasons, where months of August and January represent the two seasons respectively.

The results show that

- (1) The sea breeze starts to blow at (11:00 am), and reaches its maximum value at (4:00 pm), and minimum value at (03:00 am) and penetrates the in coastline and spreads about (100 Km), when land breeze doesn't blow.
- (2) There is no land breeze low during Summer season because of the highest temp. on the earth surface which means highest pressure on water surface.
- (3) In Winter, a land breeze blows in daytime, reaches a maximum value at (15:00 or 3:00 pm), and penetrates over water about (70 km), while at night, it reverses its direction to become a sea breeze.
- (4) We also noted that the direction of the sea breeze does not remain constant in the course of the day. It gradually veers a in clockwise direction, until by late afternoon, it blows parallel to the coastlines ,and by night becomes onshore.

References

Al-Muhyi A. A. (1998): Numerical Simulation of Local Wind-Driven Currents In Arabian Gulf,(un-pub.) Ph.D. Dissertation, University of the Philippines

- Charnock, H.** (1955). Wind stress on a water surface. Q. J. R. Meteorol. Soc. **81**, 639-640
- Deardorff, J. W.,** (1978) : Efficient Prediction of Ground Surface Temperature and Moisture, with Inclusion of a Layer of Vegetation. Journal of Geophysical Research, **83** (4c): 1889-1903.
- Estoque, M. A.,** (1960) : A Theoretical Investigation of the Sea Breeze. Quarterly Journal of the Royal Meteorological Society, **87** (372): 136-146.
- Estoque M. A. and J. M. Gross,** (1980) : Further Studies of Lake Breeze Part II : Theoretical Study. Monthly Weather Review, **109**, 619-634.
- Keyser, D., and R. A. Anthes,** (1977): The applicability of a mixed-layer model of the planetary boundary layer to real-data forecastig. Mon- Wea. Rev. **105**, 1351-1371.
- Lavoie, R.L. ,** (1972) : A Mesoscale Numerical Model of Lake-Effect Storms. Journal of the Atmospheric Sciences, **29**, 1025-1040.
- Pielke, R.A. ,** (1974) : A Comparison of Three-Dimensional and Two-Dimensional Numerical Predictions of Sea Breezes. Journal of Atmospheric Sciences, **31**: 1577-1585.
- School Atlas for Primary and Intermediate Levels,** (1985), Produced in Sweden by Esselte Map Service, Stockholm; for Secretariat of Education , SPLAJ, Sweden.
- Salem Ali Hajjaji,** (1989): The New Libya. Alfatah Universities of Al Fatah, Tiripoli
- Simpson, J. E. ,** (1994) : Sea Breeze and Local Winds. Press Syndicate of the University of Cambridge, (U.K.) pp 3-220.
- Stull, R. B.,** (1988) : An Introduction to Boundary Layer Meteorology. Kluwer Academic Publishers, U.K. pp 253-380
- Walsh, J.E. ,** (1974) : Sea Breeze Theory and Applications Journal of Atmospheric Sciences **31**: 2012-2026

Ref: 2178

Rec. 11/06/2004

In revised form 09/01/2005